# Glass composition dependence of $Eu^{3+}$ polarization in oxide glasses

**Noriyuki Wada[1], Kazuo Kojima[2], Kazuhiko Ozutsumi[2]**

**Abstract**

$Eu^{3+}$-doped borate, silicate, and phosphate glasses were prepared by the melt-quenching method. Eu $L_{III}$-edge X-ray absorption spectra were measured to study the polarization of the $Eu^{3+}$ ions in the glasses. The EXAFS analysis reveals that the nearest oxygen coordination number of the $Eu^{3+}$ ions is 6, but the actual coordination number of $Eu^{3+}$ ions is more than 6 with the additional next nearest Eu-O bonds. In the borate and silicate glasses, the nearest Eu-O distance decreased with increasing both the network modifier content and its ability. On the other hand, in the phosphate glasses, the distance tended to be constant. The electric dipole moment on an $Eu^{3+}$ ion can be evaluated from the nearest Eu-O distance and the Debye-Waller factor. It is found out that the $Eu^{3+}$ ions are more polarized with a decrease in the basicity of host glasses in which $Eu^{3+}$ ions can be dissolved homogenously.

1 *Department of Materials Science and Engineering, Suzuka National College of Technology, Shiroko, Suzuka, Mie 510-0294, Japan*

2 *Department of Applied Chemistry, Faculty of Science and Engineering, Ritsumeikan University, 1-1-1 Noji-higashi, Kusatsu, Shiga 525-8577, Japan*

## 1. Introduction

$Eu^{3+}$ ion fluoresces a red color due to the $^5D_0 \rightarrow {}^7F_2$ transition which is one of the 4f-4f transitions of the $Eu^{3+}$ ion. Therefore, the $Eu^{3+}$-doped $Y_2O_3$, $ScBO_3$, $YBO_3$, and (Gd, Y)$BO_3$ are used for red phosphors of plasma and liquid crystal displays (PD and LCD) [1-9].

$Eu^{3+}$ ions are polarized in the $Y_2O_3$ crystal since its crystal structure has no inversion center; hence, a strong red fluorescence band due to the $^5D_0 \rightarrow {}^7F_2$ electric dipole transition of the $Eu^{3+}$ ion appears at 610 - 620 nm. On the other hand, the $Eu^{3+}$ ions have the higher probability of the $^5D_0 \rightarrow {}^7F_1$ magnetic dipole transition than the probability of the $^5D_0 \rightarrow {}^7F_2$ electric dipole transition in $ScBO_3$, $YBO_3$, and (Gd, Y)$BO_3$ crystals which have inversion centers. Hence, strong orange fluorescence bands due to the $^5D_0 \rightarrow {}^7F_1$ transition appear at 580 - 600 nm.

It has been well-known that the intensities of the fluorescence band due to the electric and magnetic dipole transitions of $Eu^{3+}$ ions are changed depending on the crystal symmetry of host materials. The distortion of the local structure around $Eu^{3+}$ ions has been estimated by using the intensity ratio of the electric dipole transition to the magnetic dipole transition [10, 11]. However, there has been no report that the local structure around the $Eu^{3+}$ ion is studied by means of some direct measurements.

In this study, $Eu^{3+}$-doped oxide glasses of various types were prepared by the melt-quenching method and investigated by an X-ray absorption spectrometry to study the $Eu^{3+}$ polarization and the local structure.

## 2. Experimental Procedure

$Eu^{3+}$-doped borate, silicate, and phosphate glasses prepared in the present study are shown in Table 1. Raw materials used were $B_2O_3$ (Soekawa, 99.99 %), $SiO_2$ (Wako, 99.9 %), $NH_4H_2PO_4$ (Wako, 99.0 %), $Li_2CO_3$ (Wako, 99.0 %), $Na_2CO_3$ (Wako, 99.5 %), $K_2CO_3$ (Wako, 99.5 %), $CaCO_3$ (Wako, 99.5 %), $SrCO_3$ (Wako, 99.9 %), $BaCO_3$ (Wako, 99.9 %), $Al_2O_3$ (Wako, 99 %), and $Eu_2O_3$ (Kojundo, 99.9 %). These raw materials were weighed and mixed to obtain glasses of the compositions shown in Table 1. The powder mixture was melted using a Pt crucible for borate and silicate glasses and an alumina crucible for phosphate glass. The melting conditions for borate, silicate, and phosphate glasses were in air at 1200 ℃ for 60 min, at 1400 ℃ for 60 min, and at 1200 ℃ for 60 min, respectively. To obtain the glass, the melt was quenched by casting it on a carbon plate. This glass was crushed up using an alumina mortar and a pestle. The $Eu_2O_3$-added glass powder was melted by the same condition as the host glass. The glass was annealed for 60 min in the furnace kept at a temperature which was 20 ℃ higher than the glass

**Table 1. Glass composition, *B* value, nearest Eu-O distance (*r*), Debye-Waller factor ($\sigma$), and residual and estimated standard deviation (*R*).**

| Glass composition | *B* | *r* / pm | $\sigma$ / pm | *R* / % |
|---|---|---|---|---|
| ***Borate glasses*** | | | | |
| $60B_2O_3$-$40Li_2O$-$3.5Eu_2O_3$ (B40Li) | 0.59 | 238 | 10 | 8.0 |
| $65B_2O_3$-$35Li_2O$-$3.5Eu_2O_3$ (B35Li) | 0.52 | 237 | 10 | 9.3 |
| $70B_2O_3$-$30Li_2O$-$3.5Eu_2O_3$ (B30Li) | 0.44 | 239 | 11 | 10.2 |
| $75B_2O_3$-$25Li_2O$-$3.5Eu_2O_3$ (B25Li) | 0.37 | 241 | 12 | 10.8 |
| $80B_2O_3$-$20Li_2O$-$3.5Eu_2O_3$ (B20Li) | 0.29 | 242 | 12 | 11.2 |
| $85B_2O_3$-$15Li_2O$-$3.5Eu_2O_3$ (B15Li) | 0.22 | 243 | 12 | 12.1 |
| $90B_2O_3$-$10Li_2O$-$3.5Eu_2O_3$ (B10Li) | 0.14 | 245 | 11 | 9.8 |
| $70B_2O_3$-$30Na_2O$-$3.5Eu_2O_3$ (BNa) | 0.69 | 235 | 10 | 9.9 |
| $70B_2O_3$-$30K_2O$-$3.5Eu_2O_3$ (BK) | 0.96 | 230 | 9 | 8.2 |
| $70B_2O_3$-$30CaO$-$3.5Eu_2O_3$ (BCa) | 0.18 | 236 | 10 | 9.2 |
| $70B_2O_3$-$30SrO$-$3.5Eu_2O_3$ (BSr) | 0.22 | 234 | 12 | 12.5 |
| $70B_2O_3$-$30BaO$-$3.5Eu_2O_3$ (BBa) | 0.26 | 235 | 9 | 7.3 |
| ***Silicate glasses*** | | | | |
| $60SiO_2$-$40Li_2O$-$3.5Eu_2O_3$ (SiLi) | 0.84 | 235 | 9 | 9.2 |
| $60SiO_2$-$40Na_2O$-$3.5Eu_2O_3$ (SiNa) | 1.30 | 233 | 8 | 5.9 |
| $60SiO_2$-$20CaO$-$20Na_2O$-$3.5Eu_2O_3$ (SiCaNa) | 0.93 | 236 | 9 | 7.1 |
| $60SiO_2$-$20SrO$-$20Na_2O$-$3.5Eu_2O_3$ (SiSrNa) | 0.96 | 236 | 10 | 5.3 |
| $60SiO_2$-$20BaO$-$20Na_2O$-$3.5Eu_2O_3$ (SiBaNa) | 1.00 | 233 | 7 | 7.2 |
| ***Phosphate glasses*** | | | | |
| $60P_2O_5$-$30Li_2O$-$10Al_2O_3$-$3.5Eu_2O_3$ (PLiAl) | 0.41 | 233 | 10 | 11.2 |
| $60P_2O_5$-$30Na_2O$-$10Al_2O_3$-$3.5Eu_2O_3$ (PNaAl) | 0.66 | 235 | 9 | 7.0 |
| $60P_2O_5$-$30K_2O$-$10Al_2O_3$-$3.5Eu_2O_3$ (PKAl) | 0.93 | 236 | 9 | 9.4 |
| $60P_2O_5$-$30CaO$-$10Al_2O_3$-$3.5Eu_2O_3$ (PCaAl) | 0.14 | 233 | 9 | 8.3 |
| $60P_2O_5$-$30SrO$-$10Al_2O_3$-$3.5Eu_2O_3$ (PSrAl) | 0.18 | 234 | 10 | 7.3 |
| $60P_2O_5$-$30BaO$-$10Al_2O_3$-$3.5Eu_2O_3$ (PBaAl) | 0.22 | 234 | 11 | 14.3 |

transition temperature, and then was cooled to the room temperature at the rate of 1 ℃ /min. The disk ($\phi$ 20 mm) was formed from the powder mixture of the glass and BN (Aldrich, 99%) to measure EXAFS spectra.

EXAFS spectra for the Eu $L_{III}$-edge were taken in the transmission mode using a beam line BL-4 at the SR Center of Ritsumeikan University.

## 3. Results

The analysis of Eu $L_{III}$-edge EXAFS spectra for a reference sample $Eu_2O_3$ and (100-*x*) $B_2O_3$-*x*$Li_2O$-3.5$Eu_2O_3$ glasses has been performed as follows. The EXAFS oscillation curve, $\chi(k)$, was obtained after normalization by the sixth-order least square method and subtraction of the smooth background, where *k* is the magnitude of the wave vector of the photoelectron. The $k^3$ weighted $\chi(k)$, $k^3\chi(k)$, was Fourier transformed over the range from 38.0 to 90.0 $nm^{-1}$ in *k*. The radial structure functions, $|F(r)|$s, for the (100-*x*)$B_2O_3$-*x*$Li_2O$-3.5$Eu_2O_3$ glasses are shown in Fig. 1, where *r* is the distance from the $Eu^{3+}$ ion. In the $Eu_2O_3$, the peaks corresponding to the nearest Eu-O and Eu-Eu interactions appeared at 120 - 290 and 300 - 450 pm in *r*, respectively. In the (100-*x*)$B_2O_3$-*x*$Li_2O$-3.5$Eu_2O_3$ glasses, the peak of the nearest Eu-O interaction appeared at 120-290 pm like $Eu_2O_3$. In addition, the peak corresponding to the next nearest Eu-O interaction (290-335 pm) appeared as a shoulder of the nearest Eu-O peak. The nearest and next nearest Eu-O peaks shifted to the long distance with decreasing *x*. The area of the next nearest Eu-O peak decreased with decreasing *x*. In addition, the peaks due to the Eu-M (M: Li, B, and Eu) interactions appeared at 335-460 pm in *r*.

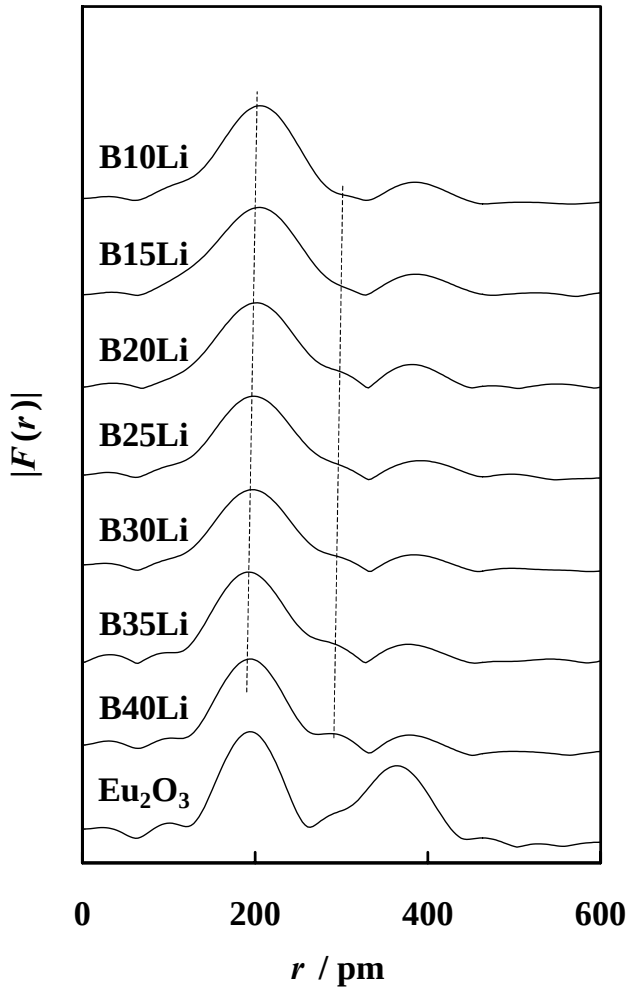


**Fig. 1. Radial structure functions, $|F(r)|$s, for Eu $L_{III}$-edge of (100-*x*)$B_2O_3$-*x*$Li_2O$-3.5$Eu_2O_3$ glasses.**

The analysis of Eu $L_{III}$-edge EXAFS spectra for the $Eu^{3+}$-doped borate, silicate, and phosphate glasses as well as the reference sample $Eu_2O_3$ has been performed in the same way as mentioned above. $|F(r)|$s for the $Eu^{3+}$-doped borate, silicate, and phosphate glasses are shown in Fig. 2 (a), (b), and (c), respectively. In all the glasses, the peak corresponding to the nearest Eu-O interaction appeared at 120 - 290 pm. In addition, the peak due to the next nearest Eu-O interaction appeared at 290 - 335 pm. In the 70$B_2O_3$-30$M_2O$-3.5$Eu_2O_3$,

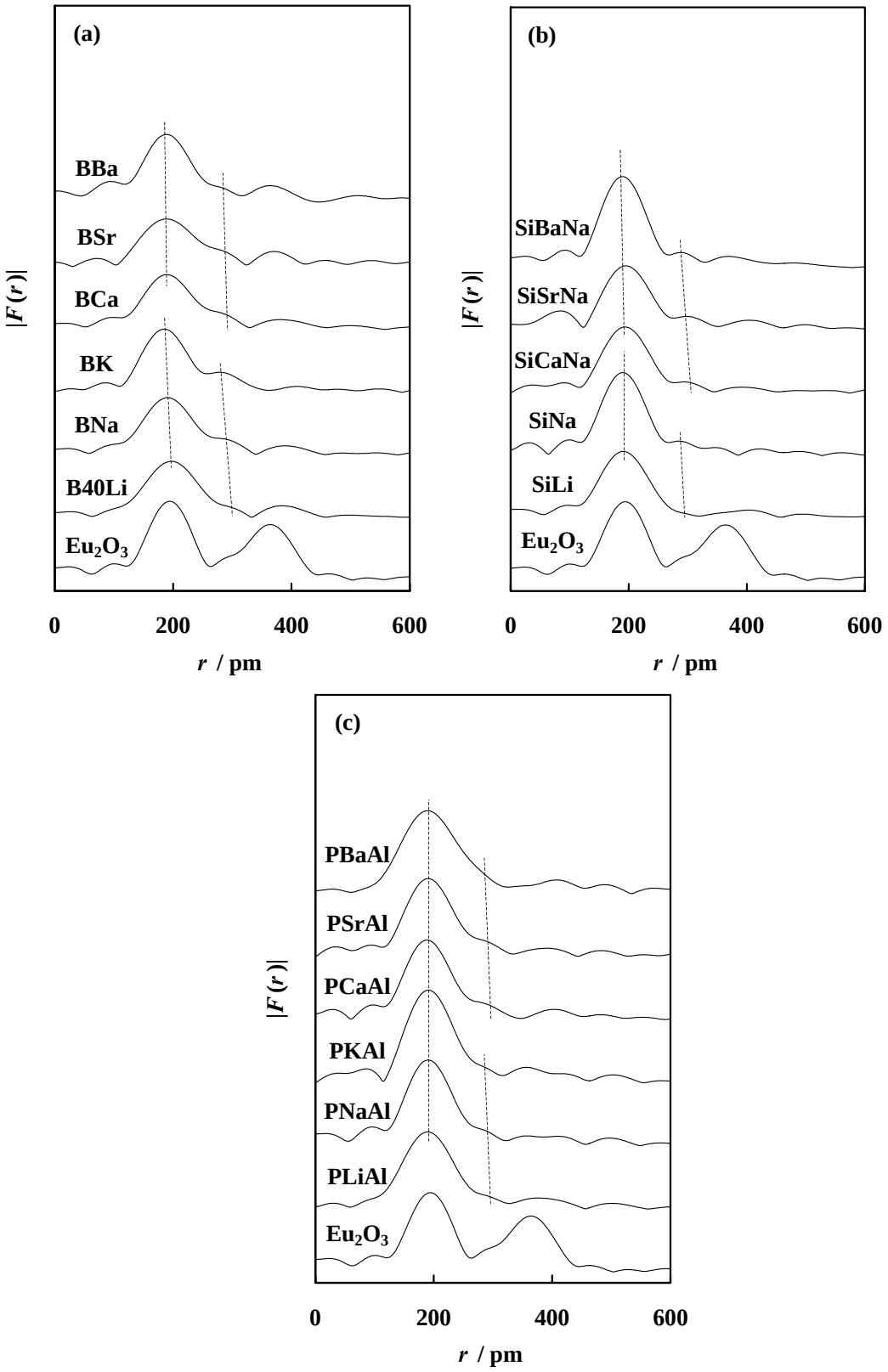


**Fig. 2. Radial structure functions, $|F(r)|$s, for Eu $L_{III}$-edge of (a) borate, (b) silicate, and (c) phosphate glasses.**

$70B_2O_3$-30M'O-$3.5Eu_2O_3$, $60SiO_2$-$40M_2O$-$3.5Eu_2O_3$, and $60SiO_2$-$20Na_2O$-20M'O-$3.5Eu_2O_3$ glasses (M: alkali metal, M' alkaline earth metal), when

the mass of M and M' increased, both Eu-O peaks shifted to the shorter distance and their area increased. In the $60P_2O_5$-$30M_2O$-$10Al_2O_3$-$3.5Eu_2O_3$ and $60P_2O_5$-$30M'O$-$10Al_2O_3$-$3.5Eu_2O_3$ glasses, when the mass of M and M' increased, the nearest Eu-O peak did not change, but the next nearest Eu-O peak shifted to the shorter distance and its area increased.

## IV. Discussion

### 4.1 Analysis of radial structure function

It can be assumed that the coordination number of $Eu^{3+}$ ions is 6 because the peak corresponding to the nearest Eu-O interaction in the $60B_2O_3$-$40Li_2O$-$3.5Eu_2O_3$ is similar to that in $Eu_2O_3$. In addition, the next nearest Eu-O peak changes by the fluctuation of $x$, and consequently, it is thought that $O^{2-}$ ions, which are away from the $Eu^{3+}$ ion, bond to the $Eu^{3+}$ ion and the coordination number of $Eu^{3+}$ ion becomes more than 6 [12-15]. Among the borate, silicate, and phosphate glasses, the number of the nearest Eu-O bond is 6, therefore, the coordination number becomes more than 6 by changing the next nearest Eu-O distance depending on the kind of M and M'. The coordination number can be actually decided by both the nearest and next nearest Eu-O peaks. However, here we have analyzed the nearest Eu-O peak in the radial structure function $|F(r)|$ using the curve-fitting method by assuming that the coordination number is 6. The results of the nearest Eu-O distances ($r_{Eu\text{-}O}$), Debye-Waller factors ($\sigma$) and residual and estimated standard deviations ($R$) are shown in Table 1. In the $(100\text{-}x)B_2O_3$-$xLi_2O$-$3.5Eu_2O_3$ glasses, the $r_{Eu\text{-}O}$ decreases with increasing $x$. The $\sigma$ has a maximum at $x$ of about 20. In the borate and silicate glasses except for the BBa glass, when the mass of M and M' increases, the $r_{Eu\text{-}O}$ decreases. On the other hand, in the phosphate glasses, the $r_{Eu\text{-}O}$ tends to be constant with increasing the mass of M and M'. In addition, in the alkali borate, silicate, and phosphate glasses, when the mass of M increases, the $\sigma$ decreases. On the other hand, in alkaline earth borate, silicate, and phosphate glasses, when the mass of M' increases, the $\sigma$ increases.

### 4.2 Glass composition dependence of $Eu^{3+}$ polarization

The $Eu^{3+}$ polarization mainly depends on the local structure around $Eu^{3+}$ ions, that is, on the distance of the nearest Eu-O bonds and coordination number of the $Eu^{3+}$ ion. In this study, the $Eu^{3+}$ polarization depends on the disorder of the nearest Eu-O distance, namely $r_{Eu\text{-}O}$ and $\sigma$, because the fitting was performed by assuming that the number of the nearest Eu-O bonds is 6. The nearest Eu-O distance is changed by the Coulomb attractive force between the $O^{2-}$ ion and the cation of the host glass, namely by the basicity of the host glass. The basicity of the host glass ($pO = -\log a(O^{2-})$, where $a(O^{2-})$ is the activity of the $O^{2-}$

ion in the host glass), can not be directly measured because the activity of the $O^{2-}$ ion bonded to some cations can not be decided. Hence, Morinaga *et al*. proposed a composition parameter *B*, which was the average basicity calculated from a glass composition [16, 17]. In the composition parameter *B*, the interaction between the cation and oxide ion, $A_i$, is given by Coulomb force as follows:

$$A_i = \frac{Z_i \times Z_{O^{2-}}}{(r_i + r_{O^{2-}})^2}. \quad (1)$$

Where $Z_i$ is the valence of the cation, $Z_{O^{2-}}$ is the valence of the $O^{2-}$ ion (= 2), $r_i$ is the radius of the cation, and $r_{O^{2-}}$ is the radius of $O^{2-}$ ion. The repulsive force $B_i^*$ is the reciprocal of $A_i$ (eq. (2)),

$$B_i^* = \frac{1}{A_i}. \quad (2)$$

A cation with higher $B_i^*$ value easily pushes the $O^{2-}$ ion away toward other cations and its oxide has higher basicity. In this study, the ionic radius reported by Shanonn [18] is used by taking into account the coordination number of the cation in a glass. The $B_i$ value is defined by eq. (3) in order to normalize the $B_{Si^{4+}}$ value of the $Si^{4+}$ ion coordinated by four $O^{2-}$ ions to be zero, and the $B_{Ca^{2+}}$ value of the $Ca^{2+}$ ion coordinated by six $O^{2-}$ ions to be 1, where the values of $B^*_{Si^{4+}} = 0.32$ and $B^*_{Ca^{2+}} = 1.38$ are calculated from eqs. (1) and (2).

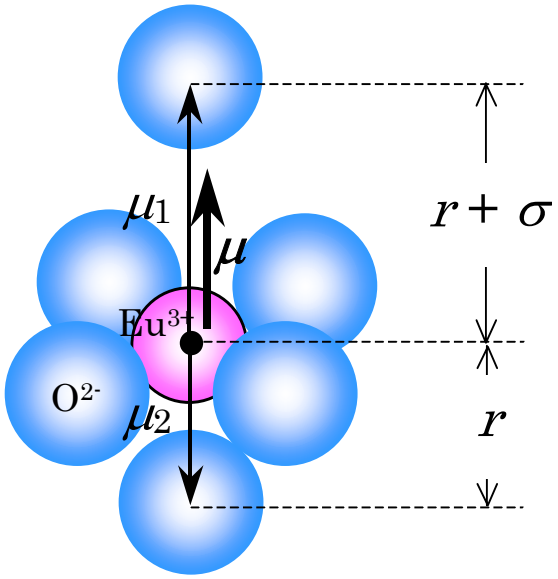


**Fig. 3. Model of electric dipole moment for an octahedron around an $Eu^{3+}$ ion.**

$$B_i = \frac{B_i^* - 0.32}{1.38}. \quad (3)$$

The *B* value of multi-component oxides was derived from $B_i$ and the cation content ratio, $n_i$.

$$B = \sum n_i \cdot B_i \quad (4)$$

The *B* values of the host glasses are shown in Table 1. The *B* values of the borate glasses were calculated considering the fraction of three- and four-coordinated boron atoms [19-22].

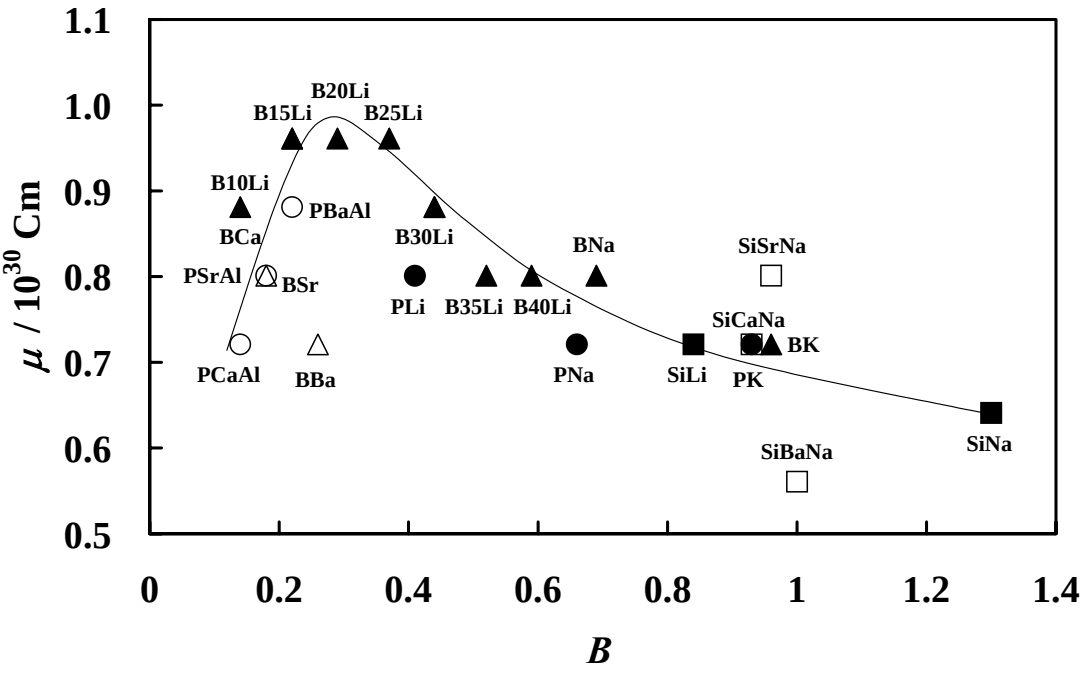


**Fig. 4. Relationship between the electric dipole moment of the $Eu^{3+}$ ion and the *B* value.**

In addition, considering the locations of the $Eu^{3+}$ ion and two $O^{2-}$ ions along the z-axis of an octahedron around the $Eu^{3+}$ ion, the electric dipole moment of the octahedron is greatest when the octahedron around the $Eu^{3+}$ ion is in such a state as shown in Fig. 3. The dipole moment can be calculated from eq. (5) using the effective charge *q*, distance vector $\boldsymbol{r}_{\text{Eu-O}}$, and Debye-Waller factor vector $\boldsymbol{\sigma}$ of the nearest Eu-O bonds.

$$\boldsymbol{\mu} = q\boldsymbol{r}_{\text{Eu-O}} + q(\boldsymbol{r}_{\text{Eu-O}} + \boldsymbol{\sigma}) \qquad (5)$$

The *B* value dependence of the calculated dipole moment, m, is shown in Fig. 4. The $Eu^{3+}$ polarization is proportional to the electric dipole moment, and hence the $Eu^{3+}$ ions are the most polarized at about 0.3 of the *B* value. The glass composition dependence of the $Eu^{3+}$ polarization is considered as follows. Generally speaking, rare earth ions cannot dissolve into the glass consisting of a glass former. Therefore, $Eu^{3+}$ ions inhomogenously dissolve into the glass having lower basicity. On the other hand, $Eu^{3+}$ ions homogenously dissolve into the glass having higher basicity. The possible local structural models of the $Eu^{3+}$ ion in a glass are suggested in Fig. 5. Below 0.3 of the *B* value, the cohered $Eu^{3+}$ ions as shown in Fig. 5 (a) are dispersing with increasing the *B* value. In addition, the $Eu^{3+}$-coordinated $O^{2-}$ ions are attracted toward the network former (NWF) and modifier (NWM) cations by the basicity of host glass, and consequently the octahedron formed by the oxygen atoms is distorted. Above 0.3 of the *B* value, the distortion of the octahedron is removing as shown from Fig. 5 (b) to (c) because the host glass is easily supplying $O^{2-}$ ions

to the $Eu^{3+}$ ion with increasing the *B* value. Therefore, it is shown that the $Eu^{3+}$ polarization can be evaluated by the analysis of the EXAFS spectrum.

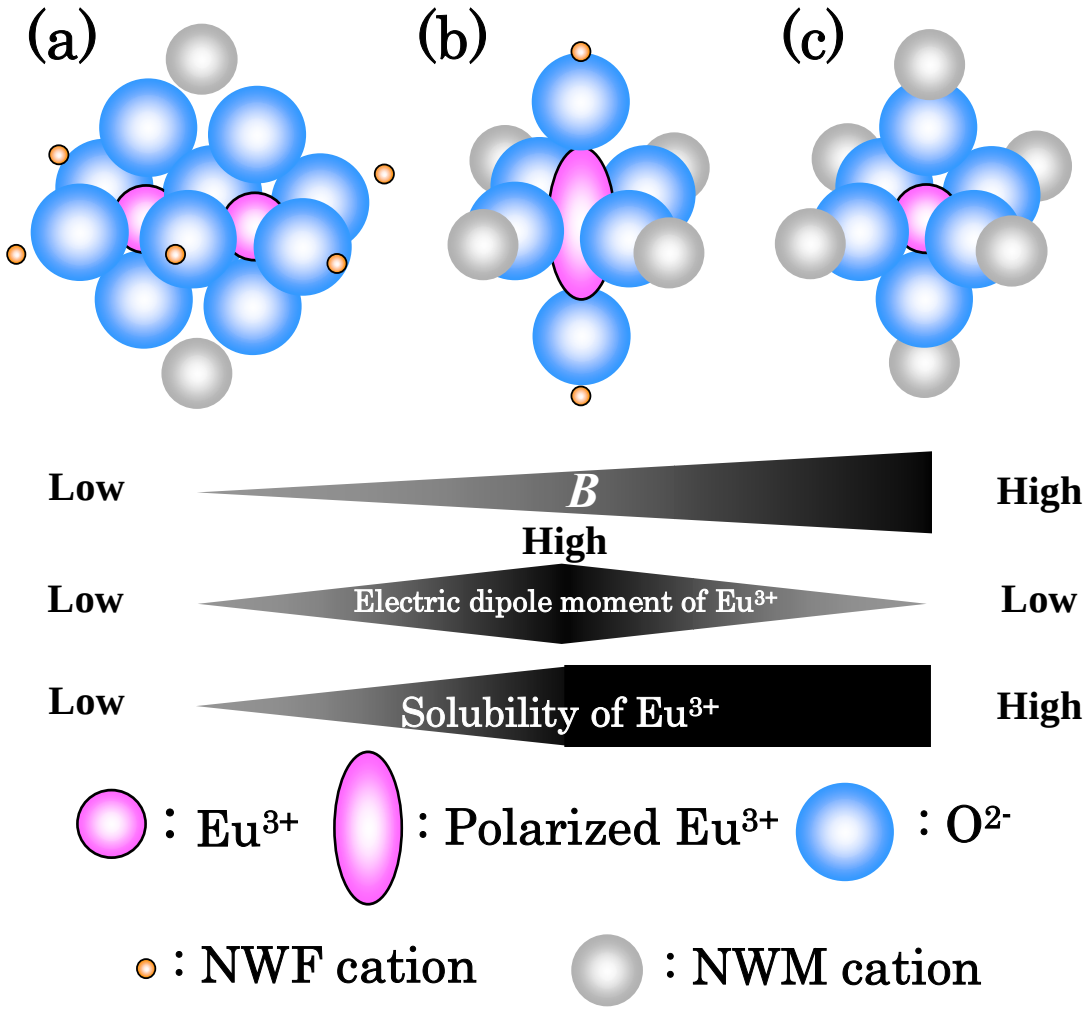


**Fig. 5. Possible local structural models around $Eu^{3+}$ ions in the oxide glasses.**

## V. Conclusion

$Eu^{3+}$-doped borate, silicate, and phosphate glasses were prepared by the melt-quenching method. The $Eu^{3+}$ fluorescence and Eu $L_{III}$-edge X-ray absorption spectra were measured to investigate the local structure around $Eu^{3+}$ ions and the $Eu^{3+}$ polarization. The EXAFS analysis reveals that the nearest oxygen coordination number of the $Eu^{3+}$ ion is 6, and the real coordination number of the $Eu^{3+}$ ion is more than 6 with the additional next nearest Eu-O bonds. In addition, in the $(100\text{-}x)B_2O_3\text{-}xLi_2O\text{-}3.5Eu_2O_3$ glasses, the nearest Eu-O distance decreased with increasing *x*. In the borate and silicate glasses except for the $70B_2O_3\text{-}30BaO\text{-}3.5Eu_2O_3$ glass, when the mass of M and M' increases, the nearest Eu-O distance decreased. On the other hand, in the phosphate glasses, the nearest Eu-O distance

tended to be constant with increasing the mass of alkali and alkaline earth metals. Furthermore, the $Eu^{3+}$ electric dipole moment can be evaluated from the distance of the nearest Eu-O bond and the Debye-Waller factor. It was found out that the $Eu^{3+}$ ions are more polarized with a decrease in the basicity of host glasses in which $Eu^{3+}$ ions can be dissolved homogenously.

**Acknowledgements**

This work was supported by the Grants-in Aid for Scientific Research (14750160) and Nanotechnology Support Project of the Ministry of Education, Culture, Sports, Science and Technology (MEXT) of Japan. Thanks are due to Prof. Tokuhiko Okamoto and Dr. Katsumi Handa at the SR Center of Ritsumeikan University for valuable comments concerning the EXAFS measurement of $Eu^{3+}$ ions in oxide glasses.

**References**

[1] K.Yokota, Shu-Xiu Zhang, K.Kimura, and A.Sakamoto, "$Eu^{2+}$-Activated Barium Magnesium Aluminate Phosphor for Plasma Displays－Phase Relation and Mechanism of Thermal Degradation," J. Lumin., **92**, 223-227 (2000).

[2] I. W. Lenggoro, B. Xia, H. Mizushima, K. Okuyama, and N. Kijima, "Synthesis of $LaPO_4$:Ce,Tb Phosphor Particles by Spray Pyrolysis," Mater. Lett., **50**, 92-96 (2001).

[3] M. Zachau, "Photocalorimetric Measurement of the Quantum Efficiencies of Phosphors," J. Lumin., **72-74**, 792-793 (1997).

[4] R. Morimo and K. Matae, "Preparation of $Zn_2SiO_4$:Mn Phosphors by Alkoxide Method," Mater. Res. Bull., **24**, 175-179 (1989).

[5] G. Blasse, B. C. Grabmaier, "Luminescent Materials," p.10. Springer-Verlag, Berlin, Germany, (1994).

[6] R. P. Rao, "Growth and Charactrization of $Y_2O_3$:$Eu^{3+}$ Phosphor Films by Sol-Gel Process," Solid State Commun., **99**, 439-443 (1996).

[7] E. P. Riedel, "Effect of Temperature on the Quantum Efficiency of $Eu^{3+}$ Flourescence in $Y_2O_3$, $ScBO_3$ and $LaBO_3$, J. Lumin., **1-2**, 176-190 (1970).

[8] J. Hao, S. A. Studenikin, and M. Cocivera, "Blue, Green and Red Cathodoluminescence of $Y_2O_3$ Phosphor Films Prepared by Spray Pyrolysis," J. Lumin., **93**, 313-319 (2001).

[9] Y. Wang, X. Guo, T. Endo, Y. Murakami, and M. Ushirozawa, "Identification of charge transfer (CT) transition in (Gd, Y)$BO_3$:Eu phosphor under 100-300 nm," J. Solid State Chem., **177**, 2242-2248 (2004).

[10] E. W. J. L. Oomen and A. M. A. van Dongen, "Europium (III) in Oxide Glasses: Dependence of the Emission Spectrum upon Glass Composition," J. Non-Cryst. Solids,

**111**, 205-213 (1989).

[11]L. D. Carlos, R. A. Sa Ferreira, V. De Zea Bermudez, C. Molina, L. A. Bueno, and S. J. L. Ribeiro, "White Light Emission of $Eu^{3+}$-Based Hybrid Xerogels," Phys. Rev., **B60**, 10042-10053 (1999).

[12] R. Anderson, T. Brennan, G. Mountjoy, R. J. Newport, and G. A. Saunders, "An EXAFS Study of Rare-Earth Phosphate Glasses in The Vicinity of The Metaphosphate Composition," J. Non-Cryst. Solids, **232-234**, 286-292 (1998).

[13] Z.-G. Wei, L.-D. Sun, X.-C. Jiang, C.-S. Liao, C.-H. Yan, Y. Tao, J. Zhang, T.-D. Hu, and Y.-N. Xie, "Correlation between Size-Dependent Luminescent Properties and Local Structure around Eu3+ Ions in YBO3:Eu Nanocrystals: An XAFS Study," Chem. Mater., **15**, 3011-3017 (2003).

[14] G. Mountjoy, J. M. Cole, T. Brennan, R. J. Newport, G. A. Saunders, and G. W. Wallidge, "A rare Earth $L_3$-Edge EXAFS and $L_1$-Edge XANES Study of Ce, Nd and Eu Phosphate Glasses and Crystals in the Composition Range from Metaphsphate to Ultraphosphate," J. Non-Cryst. Solids, **279**, 20-27 (2001).

[15] Y. Shimizugawa, J. R. Qiu, and K. Hirao, "Local Structure around Reduced Rare Earth Ions Doped in Borate Glass by XAFS," J. Non-Cryst. Solids, **222**, 310-315 (1997).

[15] H. -B. Liang, Q. Su, Y. Tao, T. -D. Hu, T. Liu, and S. L. E. Shulin, "XAFS at Eu-$L_3$ Edge and UV-VUV Excited Luminescence of Europium Doped Strontium Borophosphate Prepared in Air," J. Phys. Chem. Solids, **63**, 719-724 (2002).

[16] K. Morinaga, H. Yoshida, and H. Takebe, "Compositional Dependence of Absorption Spectra of $Ti^{3+}$ in Silicate, Borate, and Phosphate Glasses," J. Am. Ceram. Soc., **77**, 3113-3118 (1994).

[17] K. Morinaga, T. Murata, and N. Wada, "What is the Basicity of Molten Oxide?," MOLTEN SALTS, **42**, 145-156 (1999).

[18] R. D. Shannon, "Revised Effective Ionic Radii and Systematic Studies of Interatomic Distances in Halides and Chalcogenides," Acta Cryst. **A 32**, 751-767 (1976).

[19] J. Zhong and P. J. Bray, "Change in Boron Coordination in Alkali Borate Glasses, and Mixed Alkali Effects, as Elucidated by NMR," J. Non-Cryst. Solids, **111**, 67-76 (1989).

[20] S. G. Bishop and P. J. Bray, "Nuclear Magnetic Resonance Studies of Calcium Boroaluminate Glasses," Phys. Chem. Glasses, **7**, 73-81 (1966).

[21] M. J. Park and P. J. Bray, "$B^{11}$ NMR Studies of Strontium Borate Glasses and Compounds," Phys. Chem. Glasses, **13**, 50-62 (1972).

[22] S. Greenblatt and P. J. Bray, "Nuclear Magnetic Resonance Investigations of the

System BaO-$B_2O_3$," Phys. Chem. Glasses, **8**, 190-193 (1967).